Covalent Functionalization for Biomolecular Recognition on Vertically Aligned Carbon Nanofibers

Sarah E. Baker, Kiu-Yuen Tse, Eve Hindin, Beth M. Nichols, Tami Lasseter Clare, and Robert J. Hamers*

Department of Chemistry, University of Wisconsin—Madison, 1101 University Avenue, Madison, Wisconsin 53706

Received May 14, 2005. Revised Manuscript Received August 1, 2005

We compare two different strategies for covalently modifying carbon nanofibers with biological molecules such as DNA. One method begins with a photochemical reaction between the nanofibers and molecules bearing both a terminal olefin group and a protected amine group followed by deprotection to yield the free primary amine. The second method uses a chemical reaction of an aryldiazonium salt with the nanofibers followed by electrochemical reduction to the primary amine. Both methods then link the primary amines to thio-terminated DNA oligonucleotides. Our measurements show that both methods yield DNA-modified carbon nanofibers exhibiting excellent specificity and reversibility in binding to DNA probe molecules in solution having complementary vs noncomplementary sequences. Quantitative measurements show that 2.3×10^{14} DNA molecules/cm^2 will hybridize to the DNA-modified nanofiber samples, approximately eight times higher than for a flat sample of glassy carbon functionalized in an identical manner. Similar results were obtained comparing the amount of avidin that specifically binds to biotin-modified surfaces of nanofibers and glassy carbon. Our results demonstrate the ability to covalently functionalize nanofibers via two different methods that both provide excellent biomolecular recognition properties. Since the photochemical method uses molecules that are highly insulating while the diazonium method uses molecules bearing aromatic groups that are expected to be conductive, these methods can be used to prepare biologically modified nanofibers with a range of electrical properties that may be useful for electrical sensing of specific biomolecules in solution.

Introduction

The integration of nanoscale materials with biological molecules has the potential for new applications in biologically directed nanoscale assembly and in the use of nanoscale materials for biological sensing.[1,2] Nanostructured and highly porous materials, such as porous silicon and carbon, are of great interest because of their high surface area that can be used advantageously in a variety of chemical and biological sensing applications. These high surface area materials may also lead to new signal transduction processes[3,4] and to increased sensitivity in sensing applications.[5−7] Carbon-based materials are of especially great interest due to their intrinsic stability under a wide range of chemical and electrochemical conditions.[8−10]

Carbon nanofibers are a class of carbon-based materials that have several interesting features. First, they can be grown in such a way that the nanofibers are all vertically aligned.[11] When the sidewalls are electrically insulated, the ends of these vertically aligned carbon nanofiber "wires" have been used for highly sensitive detection of DNA[12] and glucose.[13] When grown as a nanofiber "forest" and not insulated, the ends and sidewalls of the nanofibers provide a very high surface area and, consequently, a very high number of biological binding sites. This high density of binding sites may increase sensitivity in the same manner as in porous materials such as porous carbon and silicon.[5−7] The nanofiber forests share some of the properties of porous carbon films, but in addition the diameter and spacing of the nanofibers can be controlled,[14] which suggests that most of the microscopic surface area can be tailored to be accessible for chemical and/or biological interactions. While many potential uses of nanofibers rely on having the fibers grown and functionalized on a solid support, it is also possible to remove

* Corresponding author: rjhamers@wisc.edu.

(1) Cui, Y.; Wei, Q.; Park, H.; Lieber, C. M. *Science* **2001**, *293*, 1289−1292.
(2) Hahm, J.; Lieber, C. M. *Nano Lett.* **2004**, *4* (1), 51−54.
(3) Dancil, K.-P. S.; Greiner, D. P.; Sailor, M. J. *J. Am. Chem. Soc.* **1999**, *121*, 7925−7930.
(4) Buriak, J. M. *Chem. Commun.* **1999**, 1051−1060.
(5) DeLouise, L. A.; Miller, B. L. *Anal. Chem.* **2004**, *76* (23), 6915−6920.
(6) Wang, J.; Chen, Q.; Renschler, C. L.; White, C. *Anal. Chem.* **1994**, *66*, 1988−1992.
(7) Lei, C.; Shin, Y.; Liu, J.; Ackerman, E. J. *J. Am. Chem. Soc.* **2002**, *124*, 11242−11243.
(8) Yang, W. S.; Auciello, O.; Butler, J. E.; Cai, W.; Carlisle, J. A.; Gerbi, J. E.; Gruen, D. M.; Knickerbocker, T.; Lasseter, T. L.; Russell, J. N., Jr.; Smith, L. M.; Hamers, R. J. *Nat. Mater.* **2002**, *1*, 253−257.
(9) Lu, M. C.; Knickerbocker, T.; Cai, W.; Yang, W. S.; Hamers, R. J.; Smith, L. M. *Biopolymers* **2004**, *73* (5), 606−613.
(10) Granger, M. C.; Witek, M.; Xu, J. S.; Wang, J.; Hupert, M.; Hanks, A.; Koppang, M. D.; Butler, J. E.; Lucazeau, G.; Mermoux, M.; Strojek, J. W.; Swain, G. M. *Anal. Chem.* **2000**, *72*, 3793−3804.
(11) Ren, Z. F.; Huang, Z. P.; Xu, J. W.; Wang, J. H.; Bush, P.; Siegal, M. P.; Provencio, P. N. *Science* **1998**, *282*, 1105−1107.
(12) Koehne, J. E.; Chen, H.; Cassell, A. M.; Ye, Q.; Han, J.; Meyyappan, M.; Li, J. *Clin. Chem.* **2004**, *50* (10), 1886−1893.
(13) Lin, Y.; Lu, F.; Tu, Y.; Ren, Z. *Nano Lett.* **2004**, *4* (2), 191−195.
(14) Melechko, A. V.; Merkulov, V. I.; McKnight, T. E.; Guillorn, M. A.; Klein, K. L.; Lowndes, D. H.; Simpson, M. L. *J. Appl. Phys.* **2005**, *97*, 041301−041339.

10.1021/cm051024d CCC: $30.25
Published on Web 09/02/2005

the nanofibers after growth and functionalization, thereby yielding large numbers of "free" functionalized nanofibers that can be later manipulated and/or assembled into more complex structures in a manner similar to many other nanomaterials.[15,16]

The successful use of carbon nanofibers for biological sensing applications relies on having chemical attachment schemes that provide stable interfaces functionalized with biomolecules of interest. Especially in a confined environment, issues of selectivity and accessibility become important. Studies on diamond thin films have established a photochemical method[8,17,18] that provides a high density of amine groups that can be used for covalent modification with DNA. More recently, an electrochemical scheme has been applied to carbon nanofibers[19] and to diamond surfaces,[20] providing the ability to achieve electrically addressable functionalization of single-walled carbon nanotubes and small bundles of vertically aligned carbon nanofibers.[19] However, the relative efficiencies of these methods have not been established. More importantly, previous studies have not quantitatively addressed the important requirement of biological specificity and accessibility that must be met in order for the unique properties of the nanofiber substrates to be fully utilized.

In this paper, we compare two different methods that can be used to modify vertically aligned carbon nanofibers (VACNFs) with DNA in order to identify whether there are significant differences in their effectiveness. Hybridization studies with complementary and noncomplementary DNA sequences are used to establish the selectivity of hybridization that results from each functionalization method. By use of on-chip fluorescence measurements as well as fluorescence wash-off measurements, we have quantitatively measured the amount of DNA that hybridizes to DNA-modified VACNFs. Comparing these results with those of similar measurements on planar samples provides a direct measure of the enhanced *biologically accessible* surface area provided by the VACNFs. Our results demonstrate that DNA-modified VACNFs exhibit very high selectivity toward complementary vs noncomplementary DNA sequences, that the hybridization is easily thermally denatured without significant degradation in binding efficiency or selectivity, and that most of the nanofiber sidewall area is accessible in hybridization studies. Overall, our results demonstrate that VACNFs provide significantly enhanced surface area with accessibility to molecules in the size range between 1 and 5 nm, thereby making them an attractive platform for integrating biological molecules with nanoscale materials.

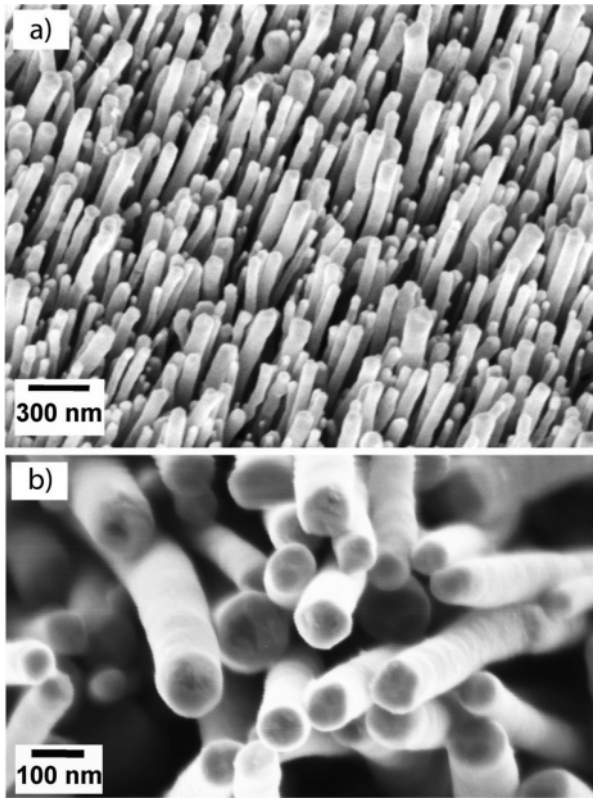

Figure 1. Scanning electron microscope images of VACNFs at low (a) and high (b) magnification.

Experimental Section

Growth. VACNFs were grown using direct current (DC) plasma-enhanced chemical vapor deposition (DC-PECVD).[21] Typical growth conditions used flow rates of 80 standard cubic centimeters per minute (sccm) ammonia and 30 sccm acetylene with a chamber pressure of 4 Torr and a DC power of 360 W. Nanofibers were grown on silicon nitride substrates that were covered with a thin film consisting of 50 nm Mo, followed by 20 nm Ti, and finally 20 nm Ni as the top layer. Figure 1a shows a scanning electron microscopy (SEM) image of the resulting carbon nanofibers. The SEM images show that the nanofibers are vertically aligned. Analysis of higher-resolution SEM images, such as that shown in Figure 1b, yield an average diameter of ~79 nm with a standard deviation of 24 nm. The length of the nanofibers can be controlled by varying the duration of the growth. Nanofibers reported here were obtained with a growth time of 15 min, which yields fibers with an average length of approximately 2 μm. On average, larger-diameter fibers are slightly longer than the smaller-diameter fibers.

Figure 2 summarizes the chemical modification scheme for covalently linking DNA to the VACNFs. We explored two different functionalization methods: a photochemical route depicted in Figure 2a and an electrochemical route depicted in Figure 2b. These methods differ only in the steps necessary to produce nanofibers functionalized with primary amines.

Photochemical Functionalization. Figure 2a depicts the photochemical functionalization of the nanofibers. Previous studies have shown that hydrogen-terminated surfaces (i.e., surfaces in which the broken bonds at the surface are terminated with H atoms) of diamond[8,9,17] and glassy carbon[22] will react with molecules containing an alkene functionality (i.e., a C═C double bond) when

(15) Smith, P. A.; Nordquist, C. D.; Jackson, T. N.; Mayer, T. S.; Martin, B. R.; Mbindyo, J.; Mallouk, T. E. *Appl. Phys. Lett.* **2000**, *77*, 1399−1401.
(16) Krupke, R.; Hennrich, F.; Kappes, M. M.; v. Löhneysen, H. *Nano Lett.* **2004**, *4*, 1395−1399.
(17) Strother, T.; Knickerbocker, T.; Russell, J. N., Jr.; Butler, J. E.; Smith, L. M.; Hamers, R. J. *Langmuir* **2002**, *18*, 968−971.
(18) Knickerbocker, T.; Strother, T.; Schwartz, M. P.; Russell, J. N., Jr.; Butler, J. E.; Smith, L. M.; Hamers, R. J. *Langmuir* **2003**, *19*, 1938−1942.
(19) Lee, C.-S.; Baker, S. E.; Marcus, M. S.; Yang, W.; Eriksson, M. A.; Hamers, R. J. *Nano Lett.* **2004**, *4* (9), 1713−1716.
(20) Yang, W.-S.; Baker, S. E.; Butler, J. E.; Lee, C.-S.; Russell, J. N., Jr.; Shang, L.; Sun, B.; Hamers, R. J. *Chem. Mater.* **2005**, *17*, 938−940.
(21) Cassell, A. M.; Ye, Q.; Cruden, B. A.; Li, J.; Sarrazin, P. C.; Ng, H. T.; Han, J.; Meyyappan, M. *Nanotechnology* **2004**, *15*, 9−15.
(22) Lasseter, T. L.; Cai, W.; Hamers, R. J. *Analyst* **2004**, *129*, 3−8.

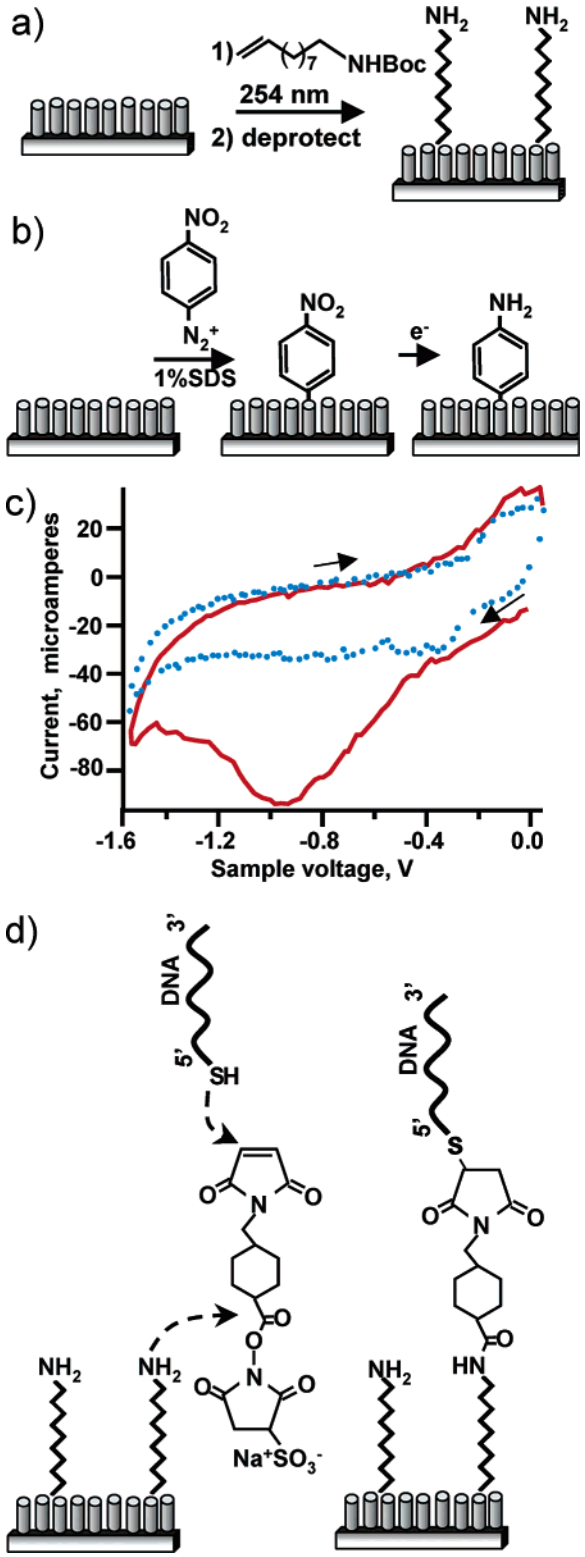

Figure 2. Functionalization of VACNFs. (a) Schematic of photochemical functionalization method to produce amino-terminated surface. (b) Schematic of electrochemical functionalization to produce amino-terminated surface. (c) Cyclic voltammograms showing the reduction of the nitro groups to amino groups. The solid line shows the first sweep starting a 0 V, down to −1.5 V, and back to 0 V. The dotted line shows a second sweep. Note the large negative peak near −1 V on the first sweep and the absence of this peak on the subsequent sweep. The sample area is approximately 0.045 cm^2. (d) Schematic of the method used to covalently link amino-modified VACNFs to thio-modified DNA.

illuminated with light at 254 nm. Here, we used an identical procedure, starting instead with VACNF forests. While no separate hydrogen-termination step was used, all experiments reported here used the VACNFs immediately after growth. Experiments using VACNFs that were exposed to ambient conditions for several days after growth yielded poor results. Previous studies have shown that the sidewalls of VACNFs are composed largely of exposed graphite edge planes, with some basal plane.[14] We presume that the atoms at the edge plane surfaces of VACNFs are also terminated with H atoms due to the highly reducing, hydrogen-rich growth environment.

As-grown VACNF forests were placed in a nitrogen-purged, quartz-covered reaction chamber, and ~5 μL of *tert*-butyloxycarbamate (tBOC) protected 10-aminodec-1-ene was dripped onto the surface, forming a liquid film over the entire surface. Each substrate was then covered with a quartz window, and the cell was purged with nitrogen for several minutes and then illuminated using 254-nm light from a low-pressure mercury lamp for 12−16 h while maintaining a steady flow of nitrogen gas. After completion of the photochemical reaction, the nonspecifically bound alkene was removed from the surface by repeatedly soaking the VACNF substrates in solvent, alternating between chloroform and methanol, for 1 h. To avoid potential complications due to water or dissolved oxygen, the tBOC-protected 10-aminodec-1-ene was stored under dry conditions and always purged with nitrogen before use. However, the influence of contaminants was not investigated.

The photochemical functionalization with the tBOC-protected 10-aminodec-1-ene was characterized using X-ray photoelectron spectroscopy (XPS); N (1s) and O (1s) of "bare" (as-grown) fibers before and after functionalization are provided in the Supporting Information. Even though the as-grown nanofibers have both N and O in them, the XPS spectra after functionalization reveal changes in the N(1s) and O(1s) regions that are characteristic of the presence of the tBOC protecting group. Additional data comparing samples that were illuminated with those that were not illuminated with 254-nm light confirmed the photochemical nature of the reaction.

The tBOC protecting group was then removed by immersing the substrate in 2 mL of a 1:1 mixture of trifluoroacetic acid:CH_2Cl_2 for 1 h and then rinsing with chloroform. Finally, the amine was neutralized by brief immersion in 10% ammonium hydroxide, leaving the surface terminated with primary amine groups.

Diazonium Functionalization. Recent studies have demonstrated that carbon nanofibers, carbon nanotubes, glassy carbon, and diamond can be functionalized by covalent grafting with the diazonium salt, 4-nitrobenzene diazonium tetrafluoroborate.[19,20,23,24] Electrochemical reduction of the nitro groups then produces surfaces terminated with primary amino (−NH_2) groups.[19,20,25] This reaction has two significant differences from the photochemical functionalization. First, the diazonium reaction links the amino group to the nanofibers via an aromatic ring, while the photochemical method typically uses an alkyl chain. Second, by selectively reducing the nitro group to an amino group under electrochemical control, the diazonium functionalization provides a pathway toward electrically addressable functionalization.[19,20]

In the diazonium method, shown in Figure 2b, the VACNF substrate is immersed in a 15 mM solution of 4-nitrobenzene diazonium tetrafluoroborate in 1% sodium dodecyl sulfate and shaken vigorously using a vortex mixer for 48 h, followed by rinsing with acetone and then water. After grafting of the nitrophenyl groups to the surface, the nitro functionality is reduced electrochemically to amino groups. While electroanalytical measurements are typically

(23) Dyke, C. A.; Tour, J. M. *Nano Lett.* **2003**, *3* (9), 1215−1218.
(24) Adenier, A.; Cabet-Deliry, E.; Chaussé, A.; Griveau, S.; Mercier, F.; Pinson, J.; Vautrin-Ul, C. *Chem. Mater.* **2005**, *17*, 491−501.
(25) Allongue, P.; Delamar, M.; Desbat, B.; Fagebaume, O.; Hitmi, R.; Pinson, J.; Savéant, J.-M. *J. Am. Chem. Soc.* **1997**, *119*, 201−207.

performed in a three-electrode geometry, in previous work we have found that a two-electrode geometry is sufficient to control the reduction of the nitro groups.[19,20] We use a similar two-electrode geometry, in which we make contact directly to the (top) metallized region of the VACNF substrate and apply a voltage to this substrate with respect to a gold wire acting as a counterelectrode. The voltage on the VACNF electrode was repeatedly swept from −0.2 to −1.8 V vs the Au electrode, in 0.1 M KCl in 10% ethanol in water. Figure 2c shows a set of voltammograms from this process. As the sample is made more negative on the first reduction sweep, the nitro groups are reduced to amino groups, resulting in a reduction peak at around −1 V. As the voltage is made more positive, no corresponding oxidation peak is observed; this indicates that once the nitro groups are reduced to amino groups, they are not easily reoxidized in aqueous solution. Subsequent voltammetry sweeps show no indication of any additional reduction or oxidation. The absence of peaks in subsequent sweeps indicates that the reduction of the nitro groups is irreversible and is completed during the first reduction sweep. While in aprotic solvents the nitro group can be reduced reversibly to the radical anion;[24] the irreversible peak observed in aqueous media demonstrates that the reduction peak is due to conversion of the nitro functionality to amine termination. Integration of the area under the first reduction peak yields 1.1×10^{16} electrons/cm^2; taking into account that 6 electrons are needed to reduce one NO_2 group via ($-NO_2 + 6H^+ + 6\ e^- \rightarrow -NH_2 + 2H_2O$) yields an amine density of 1.8×10^{15} amines/cm^2. This number is approximately 4 times higher than the value of 5×10^{14} amines/cm^2 we measured in an identical functionalization and reduction procedure on nanocrystalline diamond.[20] While measurement of the peak area has a large error associated with it, these results confirm that the VACNFs have significantly more electrically accessible surface area than a planar surface does.

DNA Covalent Linkage. Once the VACNFs are functionalized with amino groups using one of the procedures described above, subsequent chemical steps to covalently link thio-modified DNA to the VACNFs are identical. This sequence is shown in Figure 2d. As described previously,[26] the heterobifunctional cross linker sulfosuccinimidyl-4-(*N*-maleimidomethyl) cyclohexane-1-carboxylate (SSMCC), 1.5 mM in 0.1 M triethanolamine HCl buffer (pH 7), was applied to the entire amino-terminated substrate for 2 h. The substrates were then rinsed with water in order to remove excess SSMCC and then gently dried under nitrogen. To react these maleimide-terminated VACNFs with thiol-modified oligonucleotides, 1−2 μL of a 250 μM solution of 5′ thio-modified DNA was applied to the VACNF surface. This reaction was allowed to proceed for 12−16 h in a humid chamber. We will show that both the photochemical and diazonium methods produce VACNF forest substrates that are functionalized with DNA, but it should be emphasized that they differ only in the type of scaffolding introduced for amine termination at the nanofiber surface.

Characterization of DNA-Modified VACNFs. While there are many ways of characterizing the biological modification of VACNFs, the most important properties are the selectivity, accessibility, and reversibility of hybridization. To explore these properties, we functionalized each VACNF forest electrode with two sequences of DNA, denoted S1 and S2.[27] Each of these consists of a repeated sequence of 15 thymine bases that acts as a spacer, followed by 16 bases that are directly involved in hybridization. Sequences S1 and S2 differ by 4 bases. To easily functionalize two immediately adjacent regions of the sample with different DNA sequences without intermixing, we created an artificial barrier by removing the nanofibers along a narrow line using a metal spatula. When 1−2 μL of 100 μM DNA solution was then applied to each side, we found that the aqueous phase has a high affinity for the fiber-containing regions and does not wet the intermediate range where the nanofibers were removed; consequently, the different DNA solutions do not diffuse across this gap. After rinsing the nonspecifically bound DNA from the surfaces by immersing the chips in hybridization buffer (HB)[28] for 1 h, ∼10 μL of 5 μM solution of the fluorescently labeled perfect complement to S1, "F1",[29] was applied to the entire surface and allowed to hybridize for 20 min in a dark humid chamber. The chips were then immersed in 2 successive 1.5 mL solutions of HB, 5 min each, to remove any nonspecifically bound F1. After exposure to sequence F1 and removal of nonspecifically bound F1, the intensity of fluorescence from the surfaces was measured using a fluorescence microscope equipped with a high-pressure mercury lamp and appropriate filters to achieve excitation at wavelengths of 460−505 nm and measure fluorescence at 510−560 nm, optimized for the fluorescein dye.

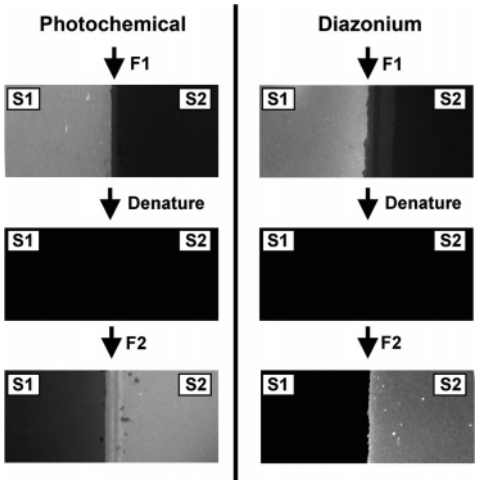

Figure 3. Fluorescence microscope images of VACNFs using two different initial functionalization methods. The left side shows VACNFs modified using the photochemical method, while the right side shows those modified using the electrochemical method; for each functionalization method, the left half of the sample was functionalized with sequence S1 and the right side was functionalized with sequence S2. The images show the intensity after hybridization with F1, denaturation, and then functionalization with sequence F2. Quantitative intensity data are shown in Table 1.

Figure 3 shows typical fluorescence microscope images of the DNA-modified nanofibers that were prepared using the photochemical method (left side), and by the diazonium method (right side), quantitative measurements of the fluorescence intensity are shown in Table 1. Figure 3 shows VACNFs after hybridization with F1 where the nanofibers on the left side of each sample were covalently linked to DNA oligonucleotide with sequence S1 and those on the right side were covalently linked to sequence S2. In both the diazonium and photochemically modified substrates, the left regions of the images are lighter, indicating fluorescence and thus the presence of F1 on the surface. The right-hand side is comparatively dark. The data show that after interaction with F1 (complementary to S1), the S1-modified side of each sample showed intense fluorescence, while the S2-modified side showed much less intensity. The sample functionalized via the diazonium method shows a slightly higher intensity than that functionalized via the photochemical method, but the difference is close to the standard deviation of the data and therefore is likely not statistically

(26) Strother, T.; Hamers, R. J.; Smith, L. M. *Nucleic Acids Res.* **2000**, *28* (18), 3535−3541.
(27) S1, 5′-HS-C6H12-T15 AA CGA TCG AGC TGC AA-3′; S2, 5′-HS-C6H12-T15 AA CGA TGC AGG AGC AA-3′.
(28) Hybridization buffer consists of 300 mM NaCl, 20 mM sodium phosphate, 2 mM EDTA, and 6.8 mM sodium dodecyl sulfate.
(29) 5′-FAM TT GCA GCT CGA TCG TT-3′.

Table 1. Fluorescence Intensity from DNA-Modified Surfaces of VACNFs Functionalized with DNA via Photochemical and Diazonium Methods, after Exposure to Fluorescently Labeled Sequences F1 (Complementary to S1), Denaturation, and Exposure to F2 (Complementary to S2)[a]

	photochemical		diazonium	
substrate	S1 modified	S2 modified	S1 modified	S2 modified
after exposure to F1	460 ± 60	85 ± 16	560 ± 80	58 ± 11
denatured	30 ± 1	30 ± 1	29 ± 1	28 ± 1
after exposure to F2	65 ± 16	410 ± 90	16 ± 6	320 ± 50

[a] The uncertainties listed are standard deviations within the imaged area.

meaningful. The similarity in fluorescence intensity from the samples modified by both functionalization methods suggests that they have nearly the same number density of DNA molecules hybridized to their surfaces. This is further verified by a more quantitative elution method described below.

To test the reversibility and stability, the substrates were denatured in water at 95 °C for three minutes. Figure 3 shows each substrate after the denaturation procedure. In both images, the S1 and S2 regions are dark. The corresponding quantitative measurements of fluorescence intensity in the images show much lower levels.

To confirm that the denaturation did not significantly degrade the nanofibers or the DNA that was covalently linked to the surface, the substrates were then immersed in F2, the complement to S2,[30] for 20 min, rinsed, and imaged as described above for hybridization to F1. Figure 3 shows the fluorescence microscope images taken of these substrates exposed to F2. These images show strong fluorescence from the right side of each sample, with only much lower intensity on the left. The images and quantitative fluorescence data indicate that F2 bound only to the region initially reacted with sequence S2, with very little or no nonspecific binding of F2 to the region originally exposed to S1. These substrates can be repeatedly hybridized and denatured as outlined above and continue to show high selectivity of the fluorescent oligonucleotide for the complementary strand tethered to the surface. Both the diazonium and photochemical methods of amine terminating the surface resulted in DNA-modified VACNFs that were highly selective toward the complement strand and highly stable to repeated hybridizations and denaturations. We note that the intensity after exposure to sequence F2 is lower than that after exposure to F1. This difference is an innate difference between the ability of the different sequences to hybridize and has also been observed on other DNA-modified surfaces.

Stability of VACNFs. Finally, we address the stability of the VACNFs. Recent studies have shown that carbon-based materials such as diamond and glassy carbon are extremely stable substrates for biosensing applications.[8] One of the potential advantages of VACNFs over other nanoscale objects used for biosensing applications, such as metal or semiconducting nanowires, for example, is that VACNFs are carbon-based materials and may have superior long-term chemical stability. We confirmed the stability of these DNA-modified VACNF substrates functionalized by either the photochemical or diazonium method by simply leaving the denatured substrates in hybridization buffer at room temperature for 10−20 days. The DNA-modified VACNFs were then immersed in either F1 or F2, and the hybridization selectivity of the complementary strand to either the S1 or S2 regions of the VACNFs was observed by fluorescence microscope. The fluorescence images indicated that each of the four substrates tested maintained selectivity toward the fluorescently labeled complementary DNA. As a comparison, we used SSMCC to link DNA (with sequence S1) to amine-terminated GAPS II glass slides (Corning). After these slides were subjected to the same conditions (10 days in hybridization buffer, two denaturations in 95 °C water), they showed no hybridization with complementary sequence F1. These data demonstrate the excellent stability of carbon nanofibers in comparison with a material commonly used as a substrate for DNA arrays.

(30) 5′-FAM-TT GCT CCT GCA TCG TT-3′.

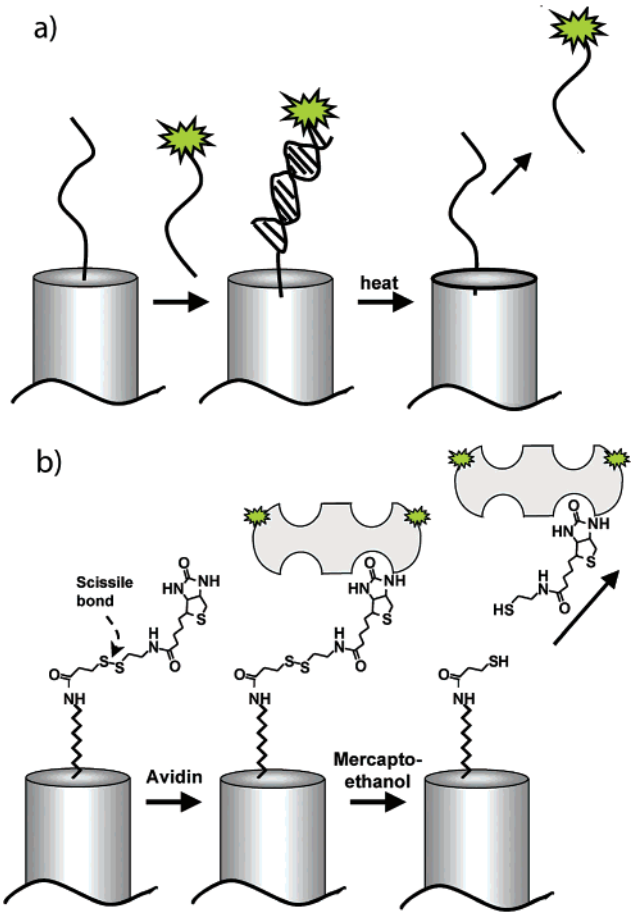

Figure 4. Schematic illustration of the wash-off methods used for quantifying the amount of biological binding to the surface. The top image shows the method for quantitative measurement of DNA hybridization. The bottom image shows a second method used for measuring the surface area, using the self-terminating adsorption of avidin onto a biotin-modified surface.

Quantitative Determination of Biologically Accessible Surface Area. One potential advantage of nanofiber forests over more conventional planar substrates is that they can provide more biological binding sites in a given geometric area, due to the three-dimensional structure of the material. To compare the amount of DNA that hybridizes to nanofiber forests functionalized by the two different methods and to quantitatively compare nanostructured vs planar surfaces, we performed two different types of experiments. Because fluorescence quenching can vary strongly depending on the electrical properties of the substrate as well as the thickness of the molecular functionalization layers, quantitative measurements of surface coverage were performed using "wash-off" experiments, in which the amount of DNA hybridized to the surface was determined by denaturing the hybridized DNA from the surface into solution and measuring the solution fluorescence. Standards made from solutions of known DNA concentration then provide a quantitative way of measuring the amount of DNA that was hybridized to the surface.

Figure 4a schematically depicts the sequence of steps used in these wash-off experiments. First, VACNF substrates of identical

Table 2. Quantitative Comparison of the Amount of DNA Hybridized to DNA-Modified Surfaces of Vertically Aligned Carbon Nanofibers, Glassy Carbon, and Diamond Surfaces

material	method	DNA molecules/cm^2	monolayer equivalent[a]
carbon nanofibers	photochemical	$(2.30 \pm 0.02) \times 10^{14}$	723%
carbon nanofibers	diazonium	$(2.32 \pm 0.02) \times 10^{14}$	729%
glassy carbon	photochemical	$(2.81 \pm 0.04) \times 10^{13}$	88%
diamond	photochemical	$(4.21 \pm 0.12) \times 10^{13}$	132%

[a] Representation in monolayer equivalent is based on a maximum packing of DNA molecules of 3.2×10^{13} cm^2. The given uncertainties reflect the maximum and minimum values obtained in repeated measurements of 2−3 samples.

area were functionalized with either the diazonium or the photochemical methods for the initial amine termination, and the reactions were carried out as described above in order to functionalize the entire surfaces with S1. After hybridization with F1 and extensive rinsing to remove physisorbed F1, the substrates were placed in 1 mL of 95 °C hybridization buffer for three minutes, and the substrates quickly removed from the liquid. At this point, all of the F1 that was hybridized to S1 on the surface should be in the liquid phase. Fluorescence microscope images of these denatured substrates show negligible fluorescence, indicating that the surface-bound F1 had indeed been removed. The concentration of F1 in each denaturing solution, and thus the number of molecules of F1 DNA initially hybridized to the surface, was determined using an ISS photon-counting fluorometer (excitation at 480 nm, collection at 521 nm, using 1-mm slits with an effective band pass of 8 nm). Calibration curves using standard fluorescein-labeled DNA solutions in the same buffer were linear over the entire range of interest, demonstrating that quenching in solution is not important at the concentrations used here.

Table 2 shows number density of DNA molecules that were hybridized to the surface. The DNA−VACNF substrates modified by both the diazonium and photochemical attachment method were hybridized to about 2.3×10^{14} F1 molecules/cm^2 based on the geometric area (i.e., the macroscopic dimensions of the sample exposed to the solution). These data indicate that both functionalization methods lead to VACNFs that have identical DNA coverage within the experimental error.

Comparison with Planar Samples. To assess the extent to which the VACNFs provide an increased number of molecules per projected surface area, we used the "wash-off" method to quantitatively compare DNA-modified VACNFs with DNA-modified planar electrodes of glassy carbon. We also compared these data to the amount of DNA hybridized to a p-type diamond thin film (on silicon substrate) that was covalently linked to DNA, because this is a carbon-based surface of intermediate roughness where the extent of the photochemical reaction has been well characterized.[8]

The glassy carbon and diamond surfaces were first terminated with hydrogen using a home-built RF hydrogen plasma chamber.[17] The glassy carbon and VACNF substrates were then functionalized simultaneously using the photochemical reaction with the tBOC-protected amino alkene, deprotected, and modified with DNA sequence S1. The diamond was also modified photochemically with a protected amino alkene, but due to specific requirements of diamond in the deprotection step, the amine used was protected with a trifluoroacetic acid (TFA) group rather than a tBOC group. After functionalization of all of the surfaces with S1 and hybridization with the fluorescently labeled complementary strand, F1, and rinsing, the complement was removed from the surface by thermal denaturation in 95 °C buffer as described above. The completeness of denaturation was again confirmed by fluorescence microscopy of the surfaces to ensure nearly complete removal of F1. Table 2 shows the results from these experiments. We note that, in this table and in subsequent discussions, all quantitative measurements of molecular densities are normalized to the geometric area of the sample and not the true surface area. The data in Table 2 show that the surfaces containing VACNFs hybridized 2.3×10^{14} DNA molecules/cm^2. In contrast, the more nearly planar samples of glassy carbon and diamond hybridized only 2.8×10^{13} (glassy carbon) and 4.2×10^{13} (diamond) molecules/cm^2, nearly an order of magnitude lower than the nanofiber samples. Previous studies on silicon have yielded densities of $(1.0-1.5) \times 10^{13}$ cm^{-2},[31] while close packing of DNA oligonucleotides would be expected to yield a density of $\sim 3 \times 10^{13}$ cm^{-2}. The difference between the amount of DNA hybridized per geometric area on the nanocrystalline diamond surfaces and glassy carbon surfaces can be correlated almost entirely to the differences in surface area associated with the roughness of the nanocrystalline diamond sample, which leads to more accessible surface area for a given sample of fixed geometric size. However, it is notable that the VACNF samples hybridized 8.2 times more DNA per unit area than the glassy carbon did and eight times more than would be expected for close packing of DNA oligonucleotides on a flat surface. These results are consistent with the expected microscopic surface area of each type of carbon surface, where the smoothest surface, glassy carbon, contained the lowest number F1 molecules on the surface, the diamond of intermediate roughness contained an intermediate number of F1 molecules per unit area, and the VACNF surface, with the highest surface area, had by far the highest coverage of F1. Though an exact determination of the relative surface areas of VACNF vs glassy carbon and polycrystalline diamond substrates is difficult to obtain, these results do imply that a significant fraction of the sidewalls of the VACNFs, and not just the ends, are functionalized by both the photochemical and diazonium reactions, and thus much of the available surface area is accessible to DNA hybridization. We conclude that the VACNFs yield approximately eight times more hybridized DNA within a given geometric area than planar substrates such as glassy carbon.

Since DNA hybridization occurs between two molecules of nearly equal diameter, it is not immediately obvious from the above studies whether the amount of DNA that will hybridize is limited by the number of DNA oligonucleotides that are covalently linked to the VACNF surface or by hybridization efficiency and/or the packing of the DNA hybridizing from solution. An alternative way of evaluating the biologically accessible sample area is to use binding of a large molecule in solution to a smaller molecule, present in large excess, that is covalently linked to the nanofiber surface. By provision of a large excess of surface binding sites (biotin groups), the number of molecules coming from the solution and binding on the surface becomes limited by the packing of the molecules adsorbing from solution; this yields an improved estimate of the accessible surface area that is less subject to possible errors arise from possible variations in the density of biomolecular binding sites on different samples. Here, we use the fact that the large protein avidin (dimensions approximately 40 Å × 50 Å × 56 Å, molecular weight ~68 000 g/ mole)[32] has a high affinity for the small molecule biotin (molecular weight 244.31). Attaching biotin to the VACNFs using a linker that has a disulfide bond gives VACNF surfaces with a large number of covalently linked biotin groups. These biotin groups will bind one monolayer of avidin molecules that can be released into solution (where they can be quantitatively measured) when the disulfide bond is cleaved, as in Figure 4b. Although the exact size of the avidin molecule on the surface is not known

(31) Chrisey, L. A.; Lee, G. U.; O'Ferrall, C. E. *Nucleic Acids Res.* **1996**, *24*, 3031−3039.
(32) Pugliese, L.; Coda, A.; Malcovati, M.; Bolognesi, M. *J. Mol. Biol.* **1993**, *231* (3), 698−710.

precisely, this method gives a very good measure of the relative surface areas of different samples and gives an absolute number of protein molecules that adsorb to the given area of the surface.

In this scheme, depicted schematically in Figure 4b, glassy carbon and VACNF samples were first photochemically modified to provide primary amino groups as described above, then reacted with a 1 mM solution of sulfosuccinimidyl 2-(biotinamido) ethyl-1,3′ dithiopropionate (Pierce) for 15 min, which links the biotin group to the surface by a linker containing a disulfide bond that can be easily cleaved. The biotin-modified surfaces were then rinsed with deionized water, dried with nitrogen, and exposed to a 0.2 mg/mL buffer solution of fluorescein-labeled avidin (Vector Labs) for an hour in a dark, humidified chamber. To remove excess avidin molecules, the samples were rinsed and immersed in 2× SSPE buffer[33] (Promega) + 1% Triton-X 100 surfactant for at least 12 h. At this point the VACNF and the glassy carbon samples are covered with a layer of avidin molecules that bind strongly to the biotin. To elute the avidin off, the different surfaces were soaked in 1.00 mL of 2× SSPE buffer (Promega) + 1% Triton-X 100 + 1% mercaptoethanol in a cuvette for at least 12 h. Mercaptoethanol is a reducing agent that cleaves the disulfide bonds in the biotin linker and hence releases the fluorescein-labeled avidin molecules into the elution buffer. The effectiveness of removal was confirmed by ensuring that little or no fluorescence remained on the surfaces after elution. The fluorescence intensity of the avidin-containing eluent was then measured with an ISS photon counting spectrofluorometer (excitation at 480 nm, collection at 515 nm, using 1-mm slits with an effective band-pass of 8 nm). The concentration of avidin in the eluent was calculated by comparing the fluorescence intensity to a calibration curve made from standards of known avidin concentration. The avidin calibration curve showed a linear dependence of fluorescence emission with concentration and a detection limit of approximately 1.4 pg/mL or 2.2 fmol/mL avidin.

These experiments indicated that the biotin-modified VACNF sample binds 1.93×10^{13} avidin molecules per cm^2 of geometric sample area. Identical measurements performed on glassy carbon surfaces yield 2.86×10^{12} avidin molecules/cm^2 (4.75 pmol/cm^2) on average, almost identical to results reported on silicon surface.[34] By assumption that avidin binds with its largest (50 Å × 56 Å) face toward the surface,[32] these numbers correspond to effective coverages of 0.78 monolayer for the glassy carbon surface and 5.4 monolayers on nanofibers. The ratio of these two numbers indicates that VACNFs have approximately seven times as much accessible area as a flat glassy carbon surface of the same dimensions. This number is nearly identical (within the experimental error) to the result obtained showing that DNA-modified VACNFs hybridize approximately eight times as much DNA as a similar flat sample.

Nanofiber electrode area was also estimated using electrical measurements of the interface capacitance. As reported elsewhere, we find that the interfacial capacitance is directly proportional to the average nanofiber length, indicating that the entire electrode area is electrically accessible. A comparison of nanofibers with flat platinum samples showed that the nanofiber samples have capacitance values approximately seven times those obtained on flat samples under identical conditions.

The DNA hybridization, protein binding, and interface capacitance measurements all indicate that the VACNF samples have approximately seven to eight times as much effective binding area as a flat sample of identical geometric dimensions. Since all three of these measurements agree, the data suggests that all of the area that is accessible to biomolecules is also accessible to ions in solution, thereby contributing to the interface capacitance. Surprisingly, however, the data obtained from analysis of SEM images is somewhat different. Analysis of SEM images suggests that the nanofiber samples should have surface area approximately 20 times that of the planar samples. Thus, while we find that the nanofiber samples have high surface area compared with planar samples, the difference is not as large as would be expected. To resolve this issue, we note that under some conditions the nanofibers can bundle together. While for small nanoscale objects such as carbon nanotubes such bundling is well known, it is also important for carbon nanofibers. SEM images of nanofiber samples before and after immersion in liquid solutions reveals that nanofibers that have been wet and then dried have pulled together presumably due to surface tension effects. While SEM images cannot be obtained while the nanofibers are in liquid solution, our data suggests that long nanofibers likely exist in a form in which at least some of them are bundled together.

Discussion

High surface area materials are of great interest for a number of applications. For applications such as sensing, these materials can provide a high number of binding sites in a given geometric sample area. This larger number of sites can lead to enhanced sensitivity for detection.[35,36] Porous materials have also been widely investigated for immobilization of enzymes.[5−7,37−40] These studies have demonstrated that immobilization of enzymes can increase their catalytic properties, but their activity is strongly affected by the morphology and size distribution of the pores[6] and by the chemical groups exposed at the surfaces of the pores.[39,40]

Carbon nanofibers present an interesting alternative to porous carbon because one can control their physical structure. In particular, the diameter and spacing between the nanofibers are controlled by the metal catalyst, while the length is controlled by the growth time. The metal catalyst can be deposited in the form of a very thin film (as used here) or using metal nanoparticles. By combination of electron-beam or optical lithography to pattern the spatial location of the catalyst, it is possible to control diameter, spacing, and length of the fibers and to vary continuously from dense nanofiber forests to individual nanofibers.[14] Previous studies of materials such as porous silica and porous carbon have shown that rigid and uniformly open porous provide an optimal geometry for interfaces to enzymes, yielding highest enzyme loading and good activity.[7] Since the average spacing between nanofibers on these substrates is approximately 150 nm and each nanofiber has a diameter of approximately 79 nm, our surfaces contain relatively large interstitial regions through which even larger proteins can move with ease. Compared with alternative porous materials,

(33) 2× SSPE buffer consists of 0.3 M NaCl, 20 mM Na_2HPO_4, and 2 mM EDTA, adjusted to pH 7.4

(34) Lasseter Clare, T.; Clare, B. H.; Nichols, B. M.; Abbott, N. L.; Hamers, R. J. *Langmuir* **2005**, *21*, 6344−6355.
(35) Pirrung, M. C. *Angew. Chem., Int. Ed.* **2002**, *41*, 1276−1289.
(36) Mishima, Y.; Motonaka, J.; Ikeda, S. *Anal. Chim. Acta* **1997**, *345*, 45−50.
(37) Singh, A. K.; Flounders, A. W.; Volponi, J. V.; Ashley, C. S.; Wally, K.; Schoeniger, J. S. *Biosens. Bioelectron.* **1999**, *14*, 703−713.
(38) Luckarift, H. R.; Spain, J. C.; Naik, R. R.; Stone, M. O. *Nature Biotechnol.* **2004**, *22*, 211−213.
(39) Sotiropoulou, S.; Gavalas, V.; Vamvakaki, V.; Chaniotakis, N. A. *Biosens. Bioelectron.* **2003**, *18*, 211−215.
(40) Gavalas, V. G.; Chaniotakis, N. A.; Gibson, T. D. *Biosens. Bioelectron.* **1998**, *13*, 1205−1211.

the open structure of the nanofibers provides a high degree of accessibility.

A second attractive aspect of carbon nanofibers is associated with the high stability of carbon-based materials.[8] Previous studies have demonstrated that covalent functionalization of diamond surfaces[8,9] and other carbon-based materials such as glassy carbon[8] yields functionalized surfaces exhibiting extraordinarily high stability, even at elevated temperatures.[9] While we have not extensively studied the stability of carbon nanofibers, we have successfully hybridized and denatured DNA-modified nanofibers; while after repeated cycles we observe some loss of intensity, our results indicate that this comes from mechanically dislodging nanofibers from the substrate rather than degradation of the surface functionalization layers.

For biosensing applications, the most relevant test of the overall chemistry is the amount of DNA that will hybridize to the DNA-modified surfaces. Our results indicate that nearly identical amounts of DNA will hybridize to surfaces modified via the photochemical and electrochemical routes. The density of atomic binding sites at the exposed surface of the nanofibers is expected to be relatively high, on the order of 10^{15} sites/cm^2. This is much higher than the density of DNA molecules that will hybridize. In previous work on planar silicon and on nanocrystalline diamond, we found that functionalization with organic molecules similar to those used here leads to molecular layers with densities of $\sim 4-6 \times 10^{14}$ cm^{-2},[17,41] close to the density of 5.4×10^{14} cm^{-2} for alkyl chains in solid *n*-$C_{33}H_{68}$.[42] These results suggest that on flat surfaces the density of the first molecular layer is primarily controlled by the packing of the molecular chains rather than the availability of surface sites for covalent attachment. Similarly, the number density of DNA molecules on flat surfaces, 2.8×10^{13} (glassy carbon) and 4.21×10^{13} (diamond) molecules/cm^2, is close to the value expected of 3.2×10^{13} cm^{-2} expected for close packing of DNA oligonucleotides. On the basis of these previous studies, we would expect the packing density of DNA molecules to depend only weakly on the number density of available surface sites for covalent attachment, provided that the latter is very high. Thus, the data in Table 2 showing that the surfaces containing VACNFs hybridized 2.3×10^{14} DNA molecules/cm^2 suggest that both methods provide amine groups with a density sufficiently high that the DNA hybridization is controlled by the maximum possible packing density of DNA molecules at the surface and not by the first functionalization layers.

While both functionalization routes lead to DNA-modified surfaces with high effective surface area, good selectivity, and good stability, one potentially important difference between the two functionalization strategies lies in the expected electrical conductivity of the molecular functionalization layer. The aromatic ring connecting the nanofibers to the amine groups is expected to be electrically conductive, while the alkyl chains from the photochemical method are insulating.[43] These differences may make one method of functionalization preferable over another for specific applications. For example, some electrical methods for detection of DNA and other biomolecules rely on electrical conductivity through a molecular layer,[44] while others make use of capacitive effects that may be better probed using a thin insulating molecular layer.[45,46] The diazonium method tethers the probe through a conductive aryl group and places the probe very near the nanofiber surface. In contrast, the photochemical method results in an insulating layer between the biological probe and the nanofiber surface. These two strategies provide a way to tailor the surface chemistry in order to maximize the electrochemical signals that may provide signatures of biological binding to the nanofibers.

Conclusions

Our results show that VACNF substrates can be effectively functionalized with biomolecules such as DNA through either a photochemical route or by a combined chemical and electrochemical route. Our results using DNA show that both methods yield a high density of biomolecular binding sites that exhibit excellent selectivity with a high degree of accessibility. Furthermore, the DNA-modified VACNFs can be denatured in hot water and rehybridized, thereby demonstrating good chemical stability. The 8-fold higher density of DNA hybridized to the nanofibers compared with planar surfaces demonstrates that most of the DNA is covalently linked to the sidewalls of the nanofibers. Similar measurements of avidin binding to biotin-modified nanofibers also show a comparable increase in biologically accessible surface area. Our results demonstrate that molecular functionalization of carbon nanofibers yields structures with excellent chemical and biological properties, making them very useful for applications such as chemical and biological sensing.

Acknowledgment. This material is based upon work supported by the National Science Foundation under Grant DMR-0210806. The authors thank Dr. Alan Cassell and Dr. Meyya Meyyappan for assistance with development of our nanofiber growth system. The first two authors contributed equally to this work.

Supporting Information Available: Nitrogen (1s) and oxygen (1s) XPS spectra of carbon nanofibers before and after photochemical functionalization with tBOC-protected 10-aminodec-1-ene. This information is available free of charge via the Internet at http://pubs.acs.org.

CM051024D

(41) Lin, Z.; Strother, T.; Cai, W.; Cao, X.; Smith, L. M.; Hamers, R. J. *Langmuir* **2002**, *18*, 788−796.
(42) Ewen, B.; Strobl, G. R.; Richter, D. *Faraday Discuss. Chem. Soc.* **1980**, *69*, 19−31.
(43) Bumm, L. A.; Arnold, J. J.; Dunbar, T. D.; Allara, D. L.; Weiss, P. S. *J. Phys. Chem. B* **1999**, *103*, 8122−8127.
(44) Willner, I.; Katz, E. *Bioelectronics: from theory to application*; Wiley-VCH: Weinheim, 2005.
(45) Yang, W. S.; Butler, J. E.; Russell, J. N., Jr.; Hamers, R. J. *Langmuir* **2004**, *20* (16), 6778−6787.
(46) Yang, W. S.; Hamers, R. J. *Appl. Phys. Lett.* **2004**, *85* (16), 3626−3628.